Nano-twinning in a γ' precipitate strengthened Ni-based superalloy

S. Y. Yuan, Z. H. Jiang, J. Z. Liu, Y. Tang & Y. Zhang

Submit your article to this journal ☒

View Crossmark data ☒

MATERIALS
RESEARCH LETTERS

Taylor & Francis
Taylor & Francis Group

ORIGINAL REPORT

OPEN ACCESS

Check for updates

Nano-twinning in a γ′ precipitate strengthened Ni-based superalloy

S. Y. Yuan[a], Z. H. Jiang[a], J. Z. Liu[a], Y. Tang[b] and Y. Zhang[a]

[a]Herbert Gleiter Institute of Nanoscience, School of Materials Science and Engineering, Nanjing University of Science and Technology, Nanjing, People's Republic of China; [b]Shanghai Institute of Applied Mathematics and Mechanics, Shanghai University, Shanghai, People's Republic of China

ABSTRACT

Twinning has been found to be a dominate mechanism in the γ′ precipitate strengthened Ni-based superalloys during service at intermediate temperatures. Here, high-resolution transmission electron microscopy and atomistic simulations have been combined to show that the twin nucleation process can be facilitated by Co replacing a fraction of Al in the γ′ precipitates, due to the negative binding energy of Co–Co atoms. The study further reveals that the presence of Co promotes a new twinning pathway featured with nucleation of one complex stacking fault (CSF) on the middle plane in between two separated CSFs.
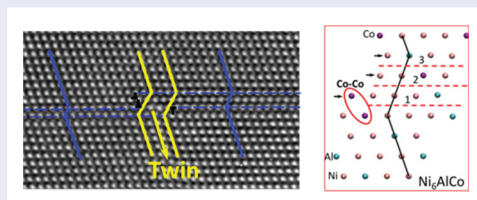
IMPACT STATEMENT

We demonstrate that Co in the γ′ precipitates promotes a new twinning pathway featured with nucleation of one CSF on the middle plane between two separated CSFs.

Twinning is generally considered as a mechanism contributing to the strength and plasticity of metallic materials, and will be facilitated under low temperatures and/or high strain-rate conditions [1,2]. Nonetheless, there exists an exception for Ni-based superalloys, which typically have ∼50% volume fraction of ordered $L1_2$ structured γ′ (Ni_3Al type) precipitates coherently embedded in the disordered face-centered cubic (fcc) γ matrix [3–7]. Deformation twinning was identified as a dominant mechanism in Ni-based superalloys during low strain rate creep and tension at a wide range of temperatures, 650–760°C [8–10], which imparts the nano-twins on the order of several to tens of atomic layers. The properties at elevated temperatures are believed to arise from the resistance of γ′ precipitates to the shear of Shockley partial dislocations and the subsequent rate-limiting process for twinning on the adjacent {111} planes in the γ′ precipitates [4–10]. Based on the limited high-resolution transmission electron microscope (HRTEM)

studies on the evolution of twins in Ni-based superalloys [6,8], it has been proposed that twin nucleation may be accomplished by successive 1/6 < 112 > Shockley partial dislocations on contiguous {111} planes. Unlike the scenario in the disordered fcc structure, gliding of 1/6 < 112 > twinning partials in the Ni_3Al-γ′ precipitates will create high energy Al–Al nearest neighbor violations at the stacking fault (SF), resulting in the formation of a complex stacking fault (CSF) [6,8,9,11]. The formation of high energy Al–Al violations suggests that the tendency for the γ′ precipitates to accommodate deformation by twinning is very low [1,12]. Obviously, this is at odds with the TEM observations of numerous nano-twins in the γ′ precipitates strengthened Ni-based superalloys [4–10,13].

In the present work, HRTEM observations and atomistic simulations are combined to demonstrate that the twin nucleation process can be facilitated by replacing a fraction of the Al atoms with Co in the Ni_3Al-γ′

Table 1. Nominal composition of the Ni-Co–Cr alloy in at.% together with compositions of γ and γ' determined by EDS in the HRTEM.

	Ni	Co	Cr	Al	Ti	Mo	W	Fe	Zr	C	B
Nominal (at.%)	48.70	22.94	15.46	5.10	4.96	1.81	0.34	0.51	0.02	0.11	0.06
γ' (at.%)	66.65	11.76	2.53	6.72	8.29	0.33	0.80	2.93	n.d.	n.d.	n.d.
$\pm S_m$	5.24	2.00	2.25	0.48	1.18	0.74	1.18	1.31	n.d.	n.d.	n.d.
γ (at.%)	44.12	30.17	16.59	1.57	1.94	1.43	1.82	2.36	n.d.	n.d.	n.d.
$\pm S_m$	1.83	2.24	1.26	1.16	1.50	1.44	1.84	0.86	n.d.	n.d.	n.d.

precipitates, which significantly reduces the chance for the formation of Al–Al bonds. Furthermore, HRTEM observations on an embryo of a three-layer twin provide the evidence of a new twinning pathway in the γ' precipitates, which is featured with nucleation of one CSF on the middle plane between two separated CSFs. This new twinning route has a lower energy barrier as compared to the classical twinning model with successive twinning partials gliding on consecutive {111} planes. Our results provide a new physical understanding on the twin nucleation process and the role of Co in the ordered L1$_2$ structured γ' precipitates of Ni-based superalloys.

The current study was performed on a γ' precipitate strengthened Nickel-based superalloy with Co, Cr, Al and Ti as the major alloying elements (see Table 1). The alloy samples were subjected to a solution anneal for 4 h at 1090°C followed by air cooling, and subsequent ageing for 24 h at 650°C and 16 h at 760°C. The resultant microstructure consists of a disordered γ matrix with ordered L1$_2$ γ' precipitates with a mean size of $\sim$50 nm. The alloy specimens with a gage section of ϕ5 mm $\times$ 25 mm were tensioned to a uniform strain of $\sim$4% with a strain rate of $8 \times 10^{-5}\,\text{s}^{-1}$ at 675°C. The TEM specimens were prepared by slicing foils from the gage along the tensile axis by wire electric discharge machining, and then mechanical grinding with SiC papers. The TEM foils were finally thinned down to electron transparency in a Struers Tenupol 5 twin jet polishing unit using an electrolyte consisting of 85% ethanol and 15% perchloric acid at a temperature of -20°C and a voltage of 20 V. HRTEM analyses were performed on a Titan G2 60-300 with an energy dispersive X-ray spectroscopy (EDS), and a Titan Cubed Themis G2 microscope operated at 300 keV. To rationalize the observed phenomenon related to the twinning at the atomic scale, we calculated the generalized stacking/planar fault energy (GSFE/GPFE) for different systems using EAM potentials [14,15] and the LAMMPS code [16].

After tension to 4% plastic strain at 675°C, the dominant substructures within grains were found to be the highly aligned, planar defects, which propagated through both the γ matrix and γ' phases. Figure 1(a) shows a bright field TEM image of the typical microstructure viewed along [011] zone axis, i.e. a high density of faulted structures, and the inserted selected area diffraction (SAD) pattern displays the superposition of the reflections from γ matrix, γ' phases, and the {111} twins, which unambiguously identifies twinning as a prevalent deformation mechanism. Close inspection of the twins in multiple grains by the HRTEM imaging reveals that nano-twinning in this γ' strengthened Ni-based alloy imparts extremely thin nano-twins, which are usually on the order of 3–20 atomic layers. An example of an HRTEM micrograph of a five-layer-thick twin shearing the γ' precipitate is shown in Figure 1(b).
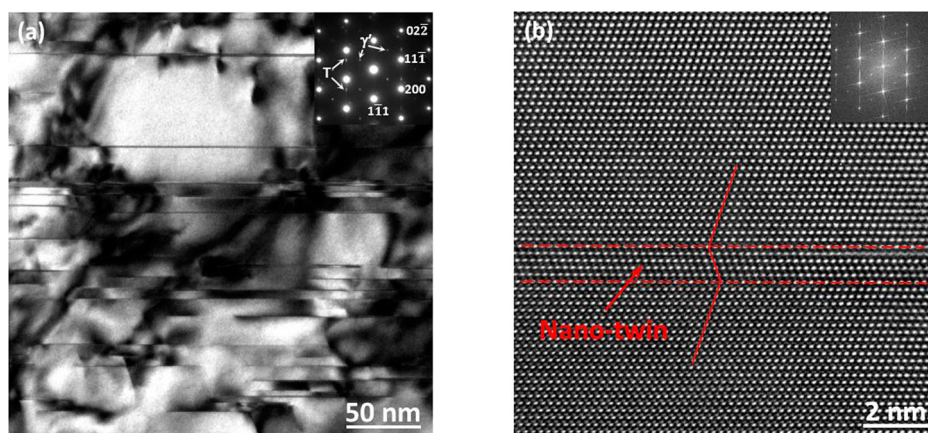

Figure 1. Typical microstructure of the deformed Ni-Co–Cr superalloy: (a) bright-field TEM image with inserted SAD, where γ' and T indicates the diffraction spots from γ' precipitates and nano-twins, respectively; (b) HRTEM image of a five-layer twin with inserted Fourier transform.
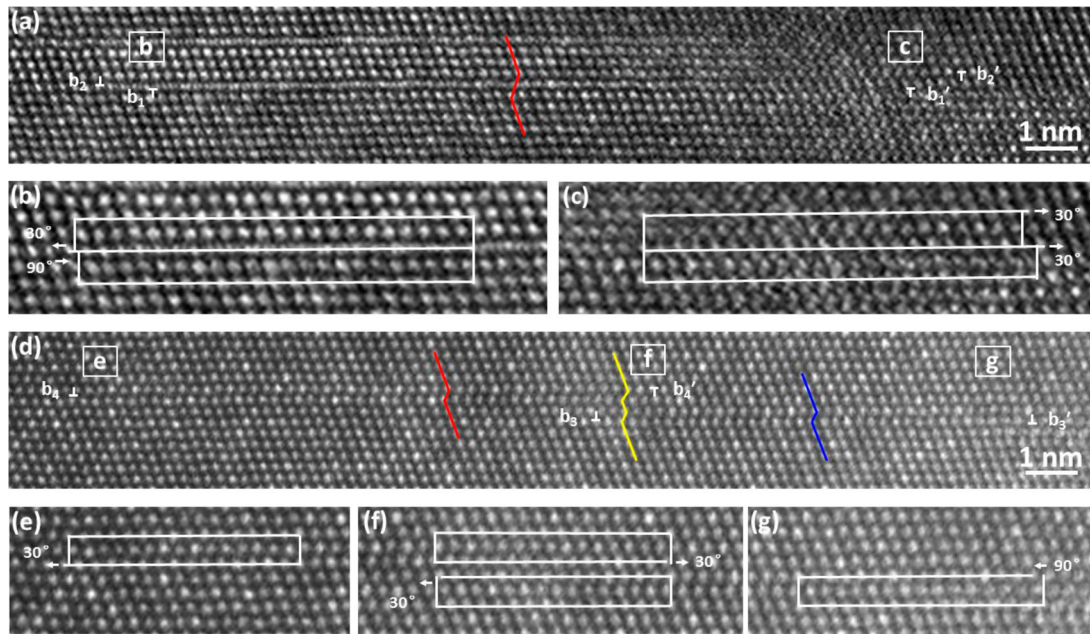
Figure 2. HRTEM images of (a) two layer CSFs and (d) two parallel CSFs on glide planes separated by one middle atomic layer. (b) and (c) Magnified images of left and right ends of the CSF in (a). (e)–(g) Magnified images of left, middle, and right section of (d).

It has been commonly believed that a nano-twin in the γ' strengthened Ni-based alloys can be nucleated through successive $1/6 < 112 >$ type of twinning partials gliding on consecutive planes [6,8,12]. In other words, a three-layer twin can be nucleated by adding one CSF immediately above or below two CSFs which serves as a nucleus [17]. Figure 2(a) shows an HRTEM image of two-layer CSFs on contiguous {111} planes. In the following analysis, **BC** in the Thompson tetrahedron is taken to be perpendicular to the page and the twin is formed by gliding of partial dislocations on the plane (a). Detailed analyses of the Burgers circuits [18,19] revealed that b_1 and b_1' are 90°, 30° ($\boldsymbol{\alpha}\mathbf{D}$, $\mathbf{C}\boldsymbol{\alpha}$) dislocations dissociated from a perfect dislocation **CD**, while b_2 and b_2' are 30°, 30° ($\boldsymbol{\alpha}\mathbf{C}$, $\mathbf{C}\boldsymbol{\alpha}$) dislocations (Figure 2(b,c)). Consequently, a three-layer twin can be initiated on the two-layer CSFs in Figure 2(a) by adding one CSF bounded by 30°, 90° ($\boldsymbol{\alpha}\mathbf{C}$, $\mathbf{D}\boldsymbol{\alpha}$) dislocations dissociated from a perfect dislocation **DC** [10]. However, it is important to note that a vast number of CSFs are also present in a pair on parallel {111} planes separated by one atomic layer rather than on neighboring planes, as shown in Figure 2(d). Unlike the two-layer CSFs, overlapping of two CSFs on parallel non-neighboring planes usually occurs only at the region where one SF gliding ahead another one, giving rise to a small overlapped area with four faulted layers, as marked by solid yellow lines in Figure 2(d). Further analysis on the Burgers circuits surrounding each end of two CSFs revealed that the CSFs are bounded by b_3, b_3' of 30°, 90° ($\boldsymbol{\alpha}\mathbf{C}$, $\mathbf{D}\boldsymbol{\alpha}$) dislocations dissociated

from a perfect dislocation **DC**, and b_4, b_4' of 30°, 30° ($\boldsymbol{\alpha}\mathbf{C}$, $\mathbf{C}\boldsymbol{\alpha}$) dislocations (Figure 2(e–g)), confirming the fact that two CSFs on non-neighboring planes are also formed by the motion of $1/6 < 112 >$ type dislocations on parallel planes separated by one middle layer. Close inspections of more than 20 CSFs in a pair revealed that two CSFs lying on non-neighboring planes separated by one middle atomic layer constitutes 48%, indicating a high probability of Shockley dislocations gliding on non-neighboring planes in the γ' strengthened Nickel alloys loaded at intermediate temperatures.

Figure 3(a) shows an example of the HRTEM image of an embryo of a three-layer twin with four atoms in length due to the approaching of three CSFs, as indicated by the yellow arrow. Analyses of Burgers circuits and atomic stacking sequences associated with the three-layer twin embryo revealed that the Burgers vectors of Shockley dislocations on the left end, i.e. b_1, b_2 and b_3, are all 30° ($\boldsymbol{\alpha}\mathbf{C}$) Shockley partials (see Figure 3(b)). The Mahajan–Chin model suggested that two 30° ($\mathbf{B}\boldsymbol{\alpha}$, $\mathbf{C}\boldsymbol{\alpha}$) and one 90° ($\mathbf{D}\boldsymbol{\alpha}$) Shockley partials were assigned to an end of a three-layer twin where the twin initiated to maintain zero net displacement at the interface [17]. The very limited HRTEM observations conducted on the dislocation configurations of the three-layer twins are also consistent with the Mahajan–Chin model [10,17]. Thus, it is unlikely that the three-layer twin embryo shown in Figure 3(a) was formed as a result of one CSF moving to the two layer CSFs on the right, given the identical dislocation assignation to the left end. A new plausible
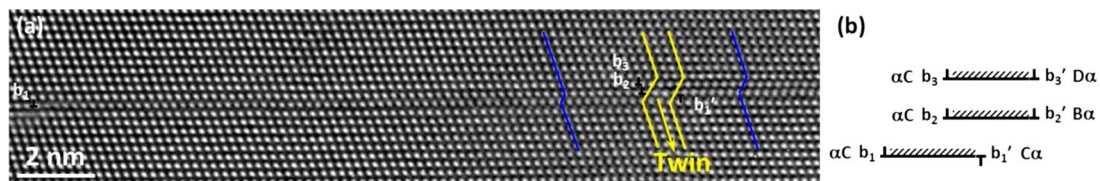
Figure 3. (a) HRTEM image of a three-layer-thick twin nucleated from two parallel CSFs on glide planes separated by one middle layer; (b) schematic of the dislocation configurations that constitute the three-layer twin in (a).

scenario for the twin nucleation we can envision is one CSF nucleated on the middle plane between CSF I and CSF III on parallel non-neighboring planes, and then followed with approaching the overlapped area of the two separated CSFs from right to left to form the twin embryo. By comparing the dislocation configurations at the ends of the twin embryo in Figure 3(a) with those of the observed two separated CSFs, it is conceivable to visualize the conversion of the two separated CSFs into a three-layer twin embryo as follows. Consider a situation of Figure 3(a) as CSF III is bounded by a 90° (**Dα**) Shockley partial on the right end which are not captured by HRTEM imaging, and consequently the dislocation configurations of CSF I and CSF III comply with those of two separated CSFs in Figure 2(d), i.e. b_1, b_1' are 30° (**αC, Cα**) Shockley dislocations, while b_3, b_3' are 30°, 90° (**αC, Dα**) Shockley partials, respectively (see Figure 3(b)). Due to the fact that the Burgers vector of the left dislocation with CSF II (b_2) is 30° (**αC**) Shockley partial, it is envisaged that the twin embryo in Figure 3(a) is formed by nucleating a CSF II bounded by 30°, 30° (**αC, Bα**) Shockley partials, which are dissociated from a perfect dislocation **BC** on the middle plane between CSF I and CSF III, as illustrated in Figure 3(b). Consequently, the total Burgers vector of the dislocations constituting the right end is equal to zero such that the three Shockley partials on the left could glide away from the junction and expand the twinned region (see Figure 3(b)). It is interesting to note that the nature of the Shockley partials constituting the ends of the three-layer twin formed via this proposed twinning route (Figure 3(b)) is same as those of Mahajan–Chin model [1,17,20].

The lattice resistance of different processes involved in twin formation can be evaluated by the concept of GSFE/GPFE [21,22], as shown in Figure 4. The simulation cell had dimensions of $15 \times 15 \times 15$ nm in the [1$\bar{1}$0], [11$\bar{2}$] and [111] crystallography orientations of the fcc lattice, respectively, and periodic boundary conditions were imposed in both the [1$\bar{1}$0] and [11$\bar{2}$] directions. The upper half was shifted relative to the lower half along the (111) plane in the [11$\bar{2}$] direction, followed by energy minimization using the EAM potentials [14,15], to calculate the GSFE/GPFE. Relaxations in [1$\bar{1}$0] and [111]

directions were all allowed. In the γ phase Ni, after the first fault is formed (denoted as route '1'), the formation of the second and third planar fault (denoted as '1-2' and '1-2-3', respectively) on successive planes are found to be easier (see Figure 4(a)). Alternatively, when the formation of the second planar fault is skipped and an SF is formed on a plane one layer above an existed SF (denoted as '1-3'), the energy required is found to be higher than that for the '1-2' and '1-2-3' processes, indicating that formation of planar faults on successive planes is energetically more favorable. Nonetheless, if two SFs separated by one atomic layer are already formed, presumably as independent nucleation events, and eventually meet/overlap as they expand, the subsequent formation of a planar fault in between them (denoted as '1-3-2') that leads to a twin nucleation is found to be much easier. Thus two different pathways for the nucleation of a twin embryo could be both operating. This is consistent with observations of nano-twins in the nanocrystalline Ni where copious grain boundaries serve as the sources for twinning partials [23]. Moreover, the twinning route 1-3-2 were observed in the nanocrystalline fcc Pt [24] and also Cu [25]. In the Ni$_3$Al-γ' phase, the opposite is found to be true (see Figure 4(b)). After the first CSF is formed, formation of second and third planar fault on successive planes and formation of a planar fault in between two CSFs separated by one atomic layer are all found to be more difficult; whereas formation of a CSF on a plane one layer above an existed CSF is found to be slightly easier. It is thus suggested that neither route 1-2 nor route 1-3 is expected to be operating, and twinning is highly unfavorable in the γ' phase, which is contrary to the experimental observations of Ni-based superalloys [4–10,13].

It is noted that adding of Al increases the stable SF energy of Ni from 134 to 210 mJ/m^2, and the energy increase actually originates from the unfavorable Al–Al bonds (also called forbidden bonds [3]) formed in the faulted structure (see Figure 4(b,d)). The formation energy of a substitutional Al in fcc Ni is negative, −0.87 eV, indicating that Al–Ni bonds is highly preferred in fcc Ni; whereas the formation energy of a pair of substitutional Al atoms in fcc Ni is −1.45 eV, indicating a positive binding energy of Al–Al atoms, 0.29 eV. This is
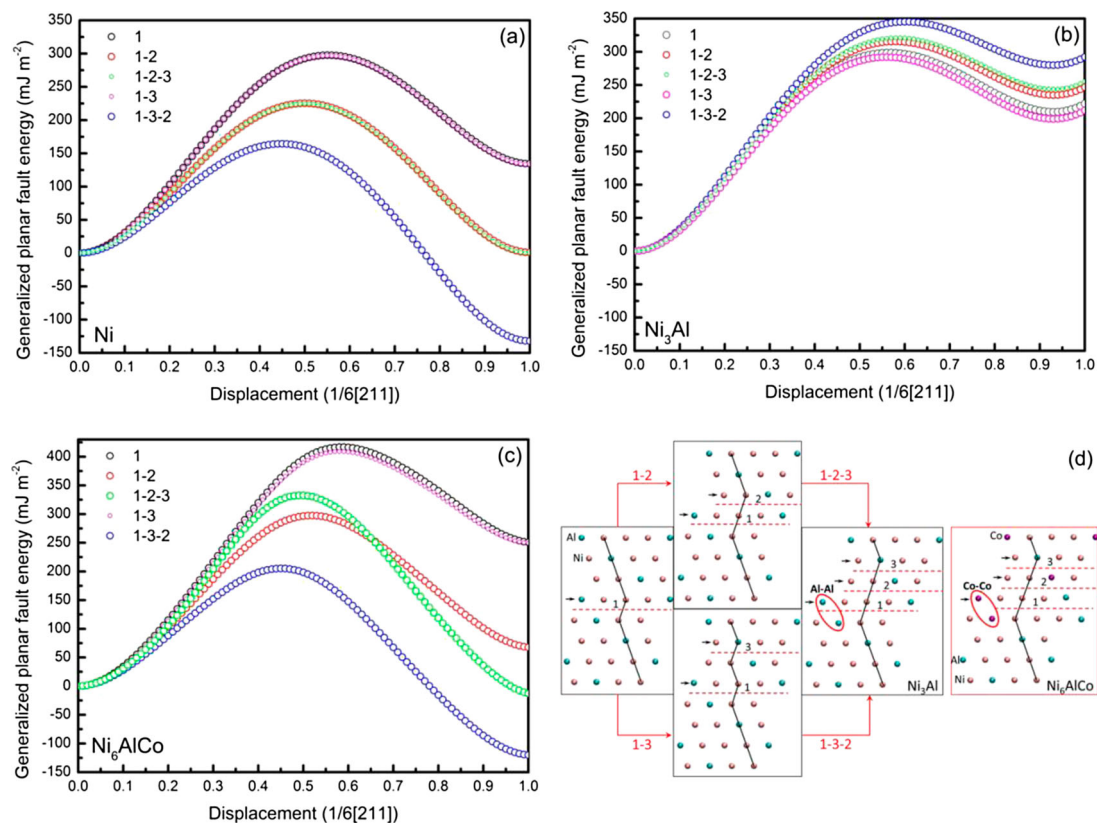
Figure 4. The calculated GPFE for various sliding sequences in (a) Ni, (b) Ni$_3$Al, and (c) Ni$_6$AlCo. (d) The atomic structures for various sliding sequences of 1, 1-2, 1-3 in Ni$_3$Al, and a three-layer twin in Ni$_3$Al and Ni$_6$AlCo, where Ni, Al and Co atom are indicated by pink, green and purple solids, respectively. The Al–Al and Co–Co bonds are outlined by red circles in the three-layer twin for Ni$_3$Al and Ni$_6$AlCo, respectively.

because the cohesive energy of fcc Al is −3.36 eV, much higher than that for fcc Ni, −4.45 eV. The positive binding energy of Al–Al atoms actually suggests that Al–Al bond is highly energetically un-preferred.

It is important to note that the actual atomic Al/Ni ratio (6.7 vs. 66.7 at.%) in the Ni$_3$Al-γ′ phase of the present alloy is not 1/3. The insufficiency of Al indicates that other alloying elements must occupy Al sites, presumably Co (11.8 at.%) and Ti (8.3 at.%). The calculation conducted on the Co (cohesive energy −4.38 eV for fcc Co) demonstrate that the formation energy of a substitutional Co in fcc Ni is also negative, −0.20 eV. On the contrary, the formation energy of a pair of substitutional Co atoms in fcc Ni is −0.61 eV, indicating a negative binding energy of Co–Co atoms, −0.21 eV. The preferred Co–Co bond actually reduces the energy of a twin structure. For example, if half of the Al atoms in Ni$_3$Al structure are randomly replaced by Co atoms to form Ni$_6$AlCo, the energies required for the twinning route of either 1-2-3 or 1-3-2 are significantly reduced, as shown in Figure 4(c–d). Therefore, both twinning mechanisms are expected to be operating again like in Ni. Furthermore, it is important to note that the twinning

route 1-3-2 has a lower energy barrier as compared to the conventional route 1-2-3, which validate the experimental observations of the new twinning pathway. The replacement of Al with Co and the negative Co–Co binding energy thus explain the high tendency for twinning in the γ′ phase of Ni-based superalloys with high content of Co in the literature [5–7,9,10].

In conclusion, HRTEM observations combined with atomistic simulations serve to illustrate that enhanced twinning tendency in γ′ phase is induced by the high content of Co replacing a fraction of Al in the Ni$_3$Al-γ′ precipitates. The replacement of Al with Co significantly reduces the chance for the formation of high energy Al–Al bonds, and the negative binding energy of Co–Co atoms considerably lowers the energy barrier for twinning in the γ′ phase. Furthermore, a fault configuration featured with two CSFs separated by one middle layer is identified as a precursor to nano-twinning, which facilitates a new twinning pathway that has a much lower energy barrier as compared to the classical one. These results provide a physical insight to tailor the performance of Ni-based superalloys at elevated temperatures through alloying, which is essential to the design of

superalloys towards more critical aero-engine applications.

Disclosure statement

No potential conflict of interest was reported by the authors.

Funding

References

[1] Christian JW, Mahajan S. Deformation twinning. Progr Mater Sci. 1995;39:1–157.
[2] Zhu YT, Liao XZ, Wu XL. Deformation twinning in nanocrystalline materials. Progr Mater Sci. 2012;57(1): 1–62.
[3] Reed RC. The superalloys fundamentals and applications. Cambridge: Cambridge University Press; 2006.
[4] Ardakani MG, Mclean M, Shollock BA. Twin formation during creep in single crystals of nickel-based superalloys. Acta Mater. 1999;47(9):2593–2602.
[5] Knowles DM, Chen QZ. Superlattice stacking fault formation and twinning during creep in γ/g′ single crystal superalloy CMSX-4. Mater Sci Eng A. 2003;340:88–102.
[6] Kovarik L, Unocic RR, Li J, et al. Microtwinning and other shearing mechanisms at intermediate temperatures in Ni-based superalloys. Progr Mater Sci. 2009;54(6):839–873.
[7] Yuan Y, Gu YF, Osada T, et al. A new method to strengthen turbine disc superalloys at service temperatures. Scr Mater. 2012;66(11):884–889.
[8] Viswanathan GB, Sarosi PM, Henry MF, et al. Investigation of creep deformation mechanisms at intermediate temperatures in René 88 DT. Acta Mater. 2005;53(10):3041–3057.
[9] Smith TM, Rao Y, Wang Y, et al. Diffusion processes during creep at intermediate temperatures in a Ni-based superalloy. Acta Mater. 2017;141:261–272.

[10] Xu YJ, Du K, Cui CY, et al. Deformation twinning with zero macroscopic strain in a coarse-grained Ni–Co–based superalloy. Scr Mater. 2014;77:71–74.
[11] Kear BH, Giamei AF. Slip and climb processes in γ′ precipitation hardened nickel-base alloys. Scr Metall. 1968;2:287–294.
[12] Kolbe M. The high temperature decrease of the critical resolved shear stress in nickel-base superalloys. Mater Sci Eng A. 2001;319-321:383–387.
[13] Barba D, Alabort E, Pedrazzini S, et al. On the microtwinning mechanism in a single crystal superalloy. Acta Mater. 2017;135:314–329.
[14] Mishin Y. Atomistic modeling of the γ and γ′-phases of the Ni–Al system. Acta Mater. 2004;52(6):1451–1467.
[15] Purja Pun GP, Yamakov V, Mishin Y. Interatomic potential for the ternary Ni–Al–Co system and application to atomistic modeling of the B2–L1$_0$ martensitic transformation. Model Simul Mater Sci Eng. 2015;23(6):065006.
[16] Plimption S. Fast parallel algorithms for short-range molecular dynamics. J Comput Phys. 1995;117:1–19.
[17] Mahajan S, Chin GY. Formation of deformation twins in F.C.C crystals. Acta Metall. 1973;21:1353–1363.
[18] Ni S, Wang YB, Liao XZ, et al. The effect of dislocation density on the interactions between dislocations and twin boundaries in nanocrystalline materials. Acta Mater. 2012;60(6–7):3181–3189.
[19] Zhao H, Song M, Ni S, et al. Atomic-scale understanding of stress-induced phase transformation in cold-rolled Hf. Acta Mater. 2017;131:271–279.
[20] Mahajan S. Critique of mechanisms of formation of deformation, annealing and growth twins: face-centered cubic metals and alloys. Scr Mater. 2013;68(2):95–99.
[21] Vítek V. Intrinsic stacking faults in body-centred cubic crystals. Philos Mag. 1968;18(154):773–786.
[22] Van Swygenhoven H, Derlet PM, Froseth AG. Stacking fault energies and slip in nanocrystalline metals. Nature Mater. 2004;3(6):399–403.
[23] Wu XL, Liao XZ, Srinivasan SG, et al. New deformation twinning mechanism generates zero macroscopic strain in nanocrystalline metals. Phys Rev Lett. 2008;100(9):095701.
[24] Wang LH, Guan PF, Teng J, et al. New twinning route in face-centered cubic nanocrystalline metals. Nature communications. 2017;8(1):2142.
[25] Wang J, Huang H. Shockley partial dislocations to twin: another formation mechanism and generic driving force. Appl Phys Lett. 2004;85(24):5983–5985.